NASA TECHNICAL MEMORANDUM

NASA TM X-73951

NASA TM X- 73951

PREDICTION OF THE ACOUSTIC IMPEDANCE OF DUCT LINERS

By

William E. Zorumski and Brian J. Tester*

September 1976

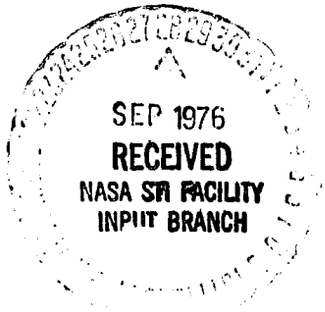

NATIONAL AERONAUTICS AND SPACE ADMINISTRATION
LANGLEY RESEARCH CENTER, HAMPTON, VIRGINIA 23665

1. Report No.	2. Government Accession No.	3. Recipient's Catalog No.
NASA TM X-73951		

4. Title and Subtitle	5. Report Date
Prediction of the Acoustic Impedance of Duct Liners	September 1976
	6. Performing Organization Code: 2610
7. Author(s): William E. Zorumski and Brian J. Tester*	8. Performing Organization Report No
	10. Work Unit No.: 505-03-21-01
9. Performing Organization Name and Address: NASA Langley Research Center, Hampton, VA 23665	11. Contract or Grant No.
	13. Type of Report and Period Covered: Technical Memorandum
12. Sponsoring Agency Name and Address: National Aeronautics and Space Administration, Washington, DC 20546	14. Sponsoring Agency Code

15. Supplementary Notes

*Consultant

16. Abstract

Recent research which contributes to the prediction of the acoustic impedance of duct liners is reviewed. This review includes the linear and nonlinear properties of sheet and bulk type materials and methods for the measurement of these properties. It also includes the effect of grazing flow on the acoustic properties of materials. Methods for predicting the properties of single or multilayered, point reacting or extended reaction, and flat or curved liners are discussed. Based on this review, methods for predicting the properties of the duct liners which are typically used in aircraft engines are recommended. Some areas of needed research are discussed briefly.

17. Key Words (Suggested by Author(s)) (STAR category underlined)	18. Distribution Statement
Duct Liners, Acoustic Impedance Noise Prediction	Unclassified Unlimited

19. Security Classif. (of this report)	20. Security Classif. (of this page)	21. No. of Pages	22. Price*
Unclassified	Unclassified	53	$4.25

*Available from { The National Technical Information Service, Springfield, Virginia 22151
STIF/NASA Scientific and Technical Information Facility, P.O. Box 33, College Park, MD 20740

CONTENTS

ABSTRACT

Recent research which contributes to the prediction of the acoustic impedance of duct liners is reviewed. This review includes the linear and nonlinear properties of sheet and bulk type materials and methods for the measurement of these properties. It also includes the effect of grazing flow on the acoustic properties of materials. Methods for predicting the properties of single or multilayered, point reacting or extended reaction, and flat or curved liners are discussed. Based on this review, methods for predicting the properties of the duct liners which are typically used in aircraft engines are recommended. Some areas of needed research are discussed briefly.

SUMMARY

The methods of predicting the acoustic properties of duct liners is reviewed. The review is divided into a discussion of typical acoustic materials and a discussion of methods of predicting the liner properties from these material properties. Acoustic materials are usually described by their acoustic impedance. For thin sheets of materials, this impedance relates the pressure differential across the material to the velocity through the material. For bulk materials, the impedance relates the pressure gradient to the velocity. There are two commonly used methods of measuring impedance. These are the standing wave method and the two microphone method. Acoustic materials exhibit significant amounts of nonlinear behavior at the high intensities usually found in aircraft engine ducts; however, this nonlinearity is well described by the measured flow resistance of the material. Also, tangential flow has a large effect on material properties. The best available information indicates that these effects can be accounted for by the material flow resistance in the presence of tangential flow. In most practical problems, it is necessary to linerize the material properties by use of an rms velocity in the material, however, this velocity must be found by an iteration procedure. Bulk materials can be characterized by two measured parameters, the impedance and wave number. The properties of complex duct liner configurations are predictable once the liner material acoustic properties are known.

SYMBOLS

a^*		acoustic resistance constant
a	$= a^*/\rho_a c_a$	
b^*		nonlinear acoustic resistance constant; liner surface radius in Equation 46
b	$= b^*/\rho_a$; $k_a b^*$	
C_D		orifice discharge coefficient
c_a		speed of sound in ambient or duct medium
D_1		distance from face of material to first minimum of Lp in standing wave measurement method
D_2		distance between minima of Lp in standing wave measurement method
d^*		liner backing cavity depth or layer thickness
d	$= k_a d^*$	
d_h^*		hole diameter of perforated sheet
d_h	$= k_a d_h^*$	
f		frequency
g^*		material acoustic reactance constant

g = $g^*/\rho_a c_a$

h^* nonlinear material acoustic reactance constant

h = h^*/ρ_a

i = $\sqrt{-1}$

K grazing flow constant

k^* wave number

k = k^*/k_a

k_a = ω/c_a

k_ω^* complex wave number constant for bulk materials

k_ω = k_ω^*/k_a

k_{rm} wave number in extended reaction liners

k_{zm} acoustic mode axial wave number in duct

L standing wave ratio, dB

Lp sound pressure level, dB re 2×10^{-5} N/m^2

ℓ^* thickness of porous or perforated sheet material

ℓ = $k_a \ell^*$

M Mach number of mean tangential, grazing or duct flow

M_ω^* material acoustic inertance

m circumferential mode number

N number of sheet material layers in a multi-layer liner

N_f number of frequency bands

$p^*(t)$ acoustic pressure

$p(t) = p^*(t)/\rho_a c_a^2$

p^* mean static pressure

$p = p^*/\rho_a c_a^2$

p^*_ω spectral (complex) acoustic pressure

$p_\omega = p_\omega^*/\rho_a c_a^2$

p_n nth harmonic of p_ω, where $\omega = n\omega_1$

$p^*_{o\omega}$ incident spectral (complex) acoustic pressure

$p_{o\omega} = p^*_{o\omega}/\rho_a c_a^2$

p^*_g grazing flow pressure fluctuations

R steady flow resistance normalized by $\rho_a c_a$

R^*_t temporal (instantaneous) acoustic resistance

$R_t = R^*_t/\rho_a c_a$

R^*_ω sheet material acoustic resistance = $Re(\Delta Z^*_\omega)$

$R_\omega = R^*_\omega/\rho_a c_a$

R_n sheet material specific acoustic resistance at nth harmonic $\omega = n\omega_1$

R_e sheet material specific acoustic resistance based on steady flow resistance, R

R_h specific orifice or hole acoustic resistance

r_e^* effective honeycomb cell radius

t^* time

$t = \omega t^*$

U^* mean tangential, grazing or duct flow velocity

$v(t)$ acoustic particle velocity normalized by c_a

v steady-flow Mach number normal to liner

v_ω^* spectral (complex) acoustic particle velocity

$v_\omega = v^*_\omega / c_a$

v_n nth harmonic of v_ω, where $\omega = n\omega_1$

v_e total effective particle velocity

X_t^* temporal (instantaneous) acoustic reactance

$X_t = \omega_r X_t^* / \rho_a c_a$

X_ω^* sheet material acoustic reactance $\equiv -\mathrm{Im}(\Delta Z_\omega^*)$

$X_\omega = X_\omega^* / \rho_a c_a$

X_n sheet material specific acoustic reactance at nth harmonic $n\omega_1$

X_e measured and/or calculated sheet material specific acoustic reactance

x^* axial coordinate in standing wave tube

ΔZ^*_ω sheet material acoustic impedance $\equiv R^*_\omega - iX^*_\omega$

$\Delta Z_\omega = \Delta Z^*_\omega / \rho_a c_a \equiv R_\omega - iX_\omega$

Z^*_t instantaneous acoustic impedance of sheet materials

Z^*_ω liner acoustic impedance = $\Delta Z^*_\omega + Z^*_{\omega_c}$ for a single layer liner

$Z_\omega = Z^*_\omega / \rho_a c_a$

ΔZ_n sheet material specific acoustic impedance at nth harmonic $n\omega_1$

$Z^*_{\omega_c}$ acoustic impedance of single-layer cavity

$Z_{\omega_c} = Z^*_{\omega_c} / \rho_a c_a$

z^*_ω spectral (complex) distributed impedance of a bulk acoustic material

$z_\omega = z^*_\omega / k_a \rho_a c_a$

α^* attenuation factor

β^* acoustic admittance

$\beta = \rho_a c_a \beta^*$

δ^* linear boundary layer thickness

δ $k_a \delta^*$

δ^*_1 boundary layer displacement thickness

$\delta_1 = k_a \delta^*_1$

λ		sound wavelength
ν		kinematic viscosity
ρ_a		density of ambient medium
ρ_e^*		sheet material effective density
ρ_e	=	ρ_e^* / ρ_a
σ		open area of perforated sheet, porosity of material
ω		circular frequency
ω_1		fundamental frequency
ω_r		reference frequency

Subscripts

i	denotes frequency band i (in place of ω)
+	refers to steady flow suction normal to the liner (i.e., from duct into liner)
-	refers to steady flow blowing normal to the liner (i.e., from liner into duct)

Superscripts

(n)	refers to nth layer in a multilayer liner
*	denotes a dimensional quantity; exceptions are the common symbols c_a, k_a, λ, ρ_a, ω.

Operators

Re, Im	real, imaginary part of
Δ	difference in a quantity
$\vec{\nabla}$	gradient vector
∇^2	divergence (gradient) or Laplacian
$\partial/\partial t$	partial differentiation with respect to time, t
Z_t^*	temporal (instantaneous) impedance operator $R_t^* + X_t^* \partial/\partial t^*$
Z_t =	$R_t + X_t \partial/\partial t$

Section 1
INTRODUCTION

Duct liners are used to reduce noise in a number of situations. One application for duct liners is the nacelles of modern aircraft engines. In this environment, the liners are exposed to high-intensity sound, (Refs. 1, 2, 3), high-speed flow, and large temperature variations. Because of non-acoustical requirements, only a few materials have ever been qualified for service in aircraft engines. A perforated sheet is one material which has been used, porous metals and rigid fiberglass sheets are others.

One goal of aircraft noise research is to develop the ability to predict the acoustical performance of new nacelle duct treatments. This prediction ability must be based on the properties of duct liners; hence, the present paper considers the subproblem of predicting the properties of duct liners. In any prediction scheme, experimental data must be included at some point, for example, the stiffness of a structure is predicted from the experimental knowledge of the modulus of elasticity from which the structure is made. Thus, part of any prediction scheme is the identification of those properties which are to be measured.

This report reviews the state of knowledge of the properties of acoustic materials and the way these properties are measured. The physical variables which affect the acoustical properties of materials are discussed and measurement methods are recommended which account for the presence of the most important physical effects. Then, methods for predicting the acoustical properties of complex duct liner configurations are given.

Section 2
ACOUSTIC MATERIALS

The propagation and attenuation of sound in lined flow ducts is understood in physical terms such that a mathematical description falls naturally into two parts. One is generally concerned with how sound that is generated within the duct propagates through the duct flow field and out through the duct termination into the far field, while the other is centered on the absorption of sound by the duct boundaries. Both areas have been studied intensively although the former has attracted more attention recently since it has been realized that the sound radiation can be sensitive to mean flow conditions within and exterior to the duct even when dissipation processes within the flow are ignored. The absorption or dissipation of acoustic energy by the lined duct surfaces is historically a well established subject, but it has been known for some time that in the present context the classical models of sound absorption must be considerably modified to take into account high-intensity sound and grazing flow effects.

In this section we are concerned with the way in which the physical process of sound absorption by an acoustic material is described through the impedance concept. In general this concept allows us to link the absorption and propagation processes without the need to consider how sound absorption is related to the physical properties of the liner materials (e.g., porosity, surface density, fiber size). That is then a separate problem which is outside the scope of the present effort, but nevertheless is one of considerable importance. We also review the largely empirical methods which attempt to represent the observed influence of sound intensity and grazing flow on the sound absorption processes through a modification of the impedance parameter. In a sense these real effects affect the convenient division of the mathematical description into two parts; that is, in practice, the absorption process cannot be specified until the local sound field is known but this depends on the propagation processes (as well as the local sound field) so that one process depends upon the other.

2.1 LINEAR IMPEDANCE

Impedance is generally defined in acoustics as the ratio of the acoustic pressure and the acoustic particle velocity at a particular frequency; (in the following it is implicit that the impedance is always a function of frequency), hence, it is in effect a vector quantity and a general property of the sound field anywhere in the duct or in the radiation field. As in linear electrical circuit theory it is a useful parameter in acoustics since the dynamics of these systems is, by definition, independent of absolute amplitudes and only the ratios of the variables are important.

2.1.1 Sheet Materials

The acoustic impedance of a material is defined in Reference 4 as the complex ratio of sound pressure to the component of particle velocity normal to the surface of the material.

$$Z^*_\omega = \frac{p^*_\omega}{v^*_\omega} = R^*_\omega - iX^*_\omega \qquad (1)$$

In equation 1, both p^*_ω and v^*_ω are understood to be the amplitude of complex harmonic motions in time with the time factor exp (- $i\omega t$). Reference 4 describes the classical impedance tube method of measuring the impedance of acoustic materials.

Equation 1 gives the total impedance at the surface of a material, such as in Figure 1a.

For thin sheets of material, it is convenient to consider the sheet to have zero thickness and define the impedance by

$$\Delta Z^*_\omega = \frac{\left[p^*_\omega(-) - p^*_\omega(+) \right]}{v^*_\omega} = \frac{\Delta p^*_\omega}{v^*_\omega} \qquad (2)$$

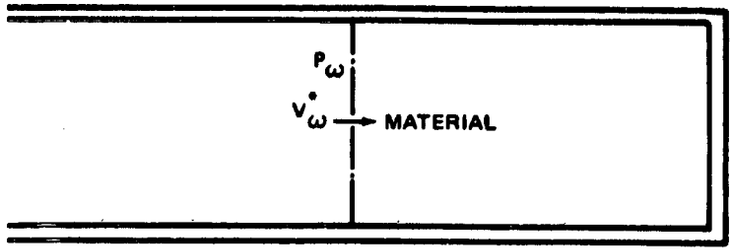

A. BULK MATERIAL SAMPLE

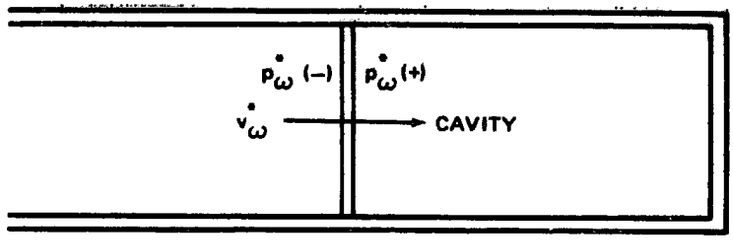

B. SHEET MATERIAL SAMPLE

Figure 1. Impedance Concepts for Bulk and Sheet Materials

This definition amounts to subtracting out the impedance of the backing cavity in Figure 1b. This backing impedance is approximately i cot (k* d*), where d* is the backing depth.

At sufficiently low sound pressure levels the impedance of a thin sheet is of the form

$$\Delta Z^*_\omega = R^*_\omega - i\omega M^*_\omega$$

where M^*_ω, the material inertance, is usually a fairly weak function of frequency; both R^*_ω and X^*_ω are a function of the material geometry and the mean properties of the local fluid, e.g., its coefficient of viscosity and mean density as well as frequency. Thus, although ΔZ^*_ω can be measured quite easily, data should be corrected if fluid properties in the measurement and application environments are significantly different. It is beyond the scope

of the present report to review the functional dependence of ΔZ_ω^* on the material geometry and the fluid's mean properties although it is given when we consider the special case of perforate materials below since it is of a particularly simple form.

2.1.2 Bulk Materials

Scott (Reference 5) has shown that the propagation of sound waves in isotropic porous materials can be characterized by two complex constants. Scott used a complex wave number and density; however, other pairs of constants may be used also. For example, Bies (Reference 6, ch. 10) uses a complex propagation constant and characteristic impedance to characterize bulk materials.

In this report, we will use a distributed impedance, or impedance per unit length, to relate the pressure gradient to the velocity in an isotropic porous medium.

$$\vec{\nabla} p_\omega^* + z_\omega^* v_\omega^* = 0 \tag{3}$$

The form of equation 3 is used here because of the analogy to equation 2. The gradient of pressure is approximated by $-\Delta p_\omega^* / \ell^*$ where ℓ^* is the thickness of a thin sample such as in Figure 1b. Equation 3, together with the wave equation given by Scott (Reference 5).

$$\nabla^2 p_\omega^* + k_\omega^{*2} p_\omega^* = 0 \tag{4}$$

completely describe the properties of waves in infinite media, porous or otherwise. In the limit of 100 percent porosity the porous medium is the ambient medium and then

$$k_\omega^* = \omega / c_a \tag{5}$$

which is a real number, and

$$z^*_\omega = -i\omega\rho_a \qquad (6)$$

which is a negative imaginary number.

2.1.3 Measurement Methods

The simplest method of measuring the impedance of a material is the standing wave method described in Reference 4. Figure 2 (from Reference 4) shows the apparatus for this measurement.

This method is attractive because it does not require a lot of sophisticated equipment for its use. A speaker, driven by an audio oscillator (and perhaps an amplifier) sets up a standing wave pattern in the tube in which the sample is placed. The experimenter moves the microphone away from the sample face, noting the minimum sound pressure level L_p (D_1), the distance to that minimum D_1, the maximum level L_p (D_1) $+L$, and the distance between minima D_2. From these measurements, and the assumption that the waves in the tube are of the form exp $\{\pm ik^*x^*\}$ the impedance of the sample may be deduced.

CR48

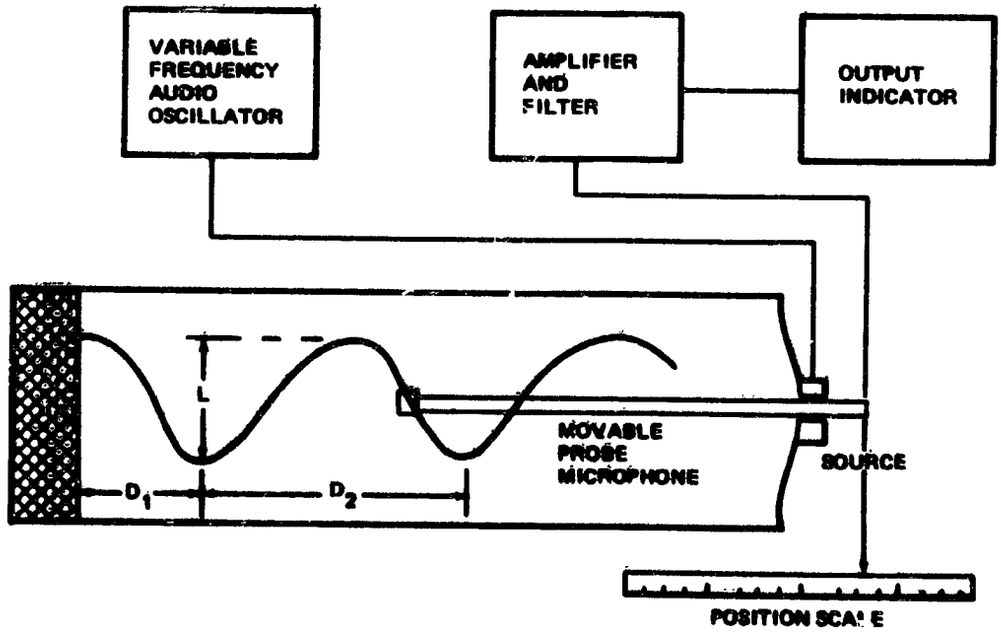

Figure 2. Apparatus for Standing-Wave Method of Measuring Material Impedance

One difficulty which occurs with the standing wave method is that the effective wave number k* is not real due to absorption of sound by the tube walls. This situation was analyzed by Lippert (Reference 7) who considered waves in the tube of the form exp $\{\pm(ik^* x^* + \alpha^* x^*)\}$ where α^* is an attenuation factor due to the tube walls. In this case, it is necessary to determine the envelope of the pressure minima, as shown in Figure 3, to correctly find the impedance of the material.

Thin sheet materials are characterized by the impedance which is given by Equation 2. This impedance is found, using the standing wave method, by subtracting the impedance of the backing cavity (Figure 1b) from the impedance of measured impedance. Since the impedance of the backing cavity is approximately i cot d, where d is the cavity depth, the measured impedance is large when d is near $n\pi$, n = 1, 2... The measured impedance in front of the saraple is consequently large and the sample inpedance, which is found by taking the difference between two large numbers, will not be accurate. The obvious solution to this problem is to hold d at $\pi/2$ (the quarter-wave cavity) such that the cavity impedance is zero and the measured impedance is the material

CR48

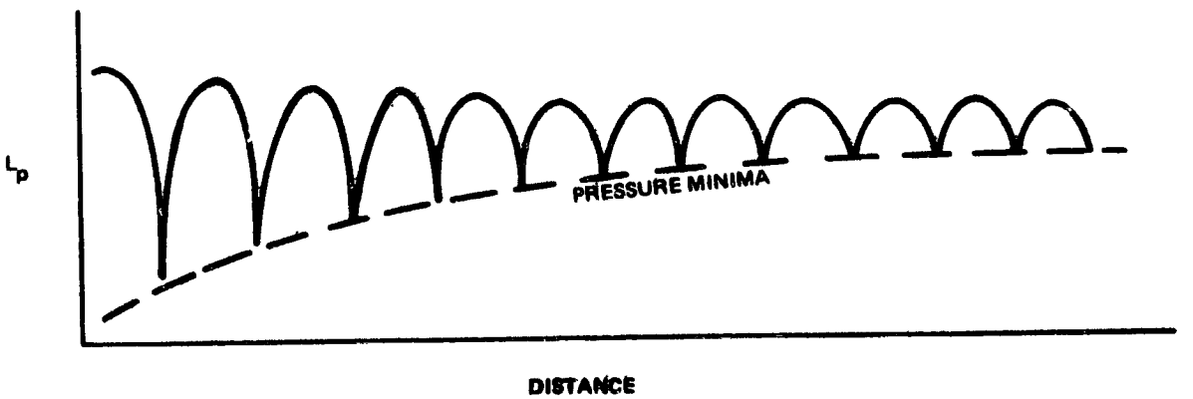

Figure 3. Typical Standing-Wave Pattern with Tube Wall Absorption Effects

impedance. While this is simple as a mathematical concept, it introduces the practical difficulty of adjusting the cavity depth to $\lambda/4$ for each test frequency.

A second method for measuring the impedance of a thin sheet is the two-microphone method. As the name implies, an additional microphone is added to the test apparatus in Figure 2. This microphone is fixed at the end of the cavity and provides a measure of both the velocity through the thin sample and the pressure immediately behind the sample. The method also requires an additional piece of equipment, a phase meter, to determine the complex ratio of the pressure in front of the sample to the pressure at the wall of the backing cavity.

Melling (Reference 8) has given an extensive discussion of the design and operation of a precision impedance tube using the standing wave method of measurement.

Melling also provides a brief discussion of the two-microphone method and notes that its principal difficulties are errors in phase measurement, which is an instrumentation problem rather than a fundamental defect of the method, and errors due to placing one microphone at the face (in front of) the sample. Melling was studying the impedance of perforated sheets and the pressure field in the neighborhood of an array of orifices is very nonuniform. This problem can be overcome by moving the microphone back from the sample face a fraction of a wavelength. When this is done, the formula for the impedance of the sheet is slightly more complex than if the microphone were right at the sheet face, but the sheet impedance is still given as a function of the complex pressure ratio between the microphones. Like the standing wave method, the two microphone method works best when the backing cavity is one-quarter wavelength in depth.

Bulk materials must be characterized by two complex constants, as shown by Scott in Reference 5. There is a wide range of choices available for which two constants are used, such as compressibility, sound speed, wave number, characteristic impedance, or distributed impedance, however, there are only two independent constants. We have arbitrarily selected the

wave number (Equation 4) and the distributed impedance (Equation 3) for use in this report. Since there are two independent complex constants which characterize the material, at least four physical quantities related to the material sample must be measured. Scott (Reference 5) obtained the complex wave number (propagation constant) by moving a microphone through the bulk material while observing the signal of the microphone output and the signal from the driving oscillator on a dual beam oscilloscope. Figure 4 shows a schematic of Scott's apparatus. The wave length was found by moving the microphone until 360° phase shift occurred, and the attenuation of the wave could be observed by the change of the microphone output as a function of distance. These two constants are easily related to the complex wave number of the material. A modern version of Scott's experiment would use a two microphone technique with a phase meter used to determine the wavelength. The second complex constant used by Scott to characterize the material was the characteristic impedance. This is the impedance at the front of an infinitely deep sample of the material which can be measured by the standing wave method.

CR48

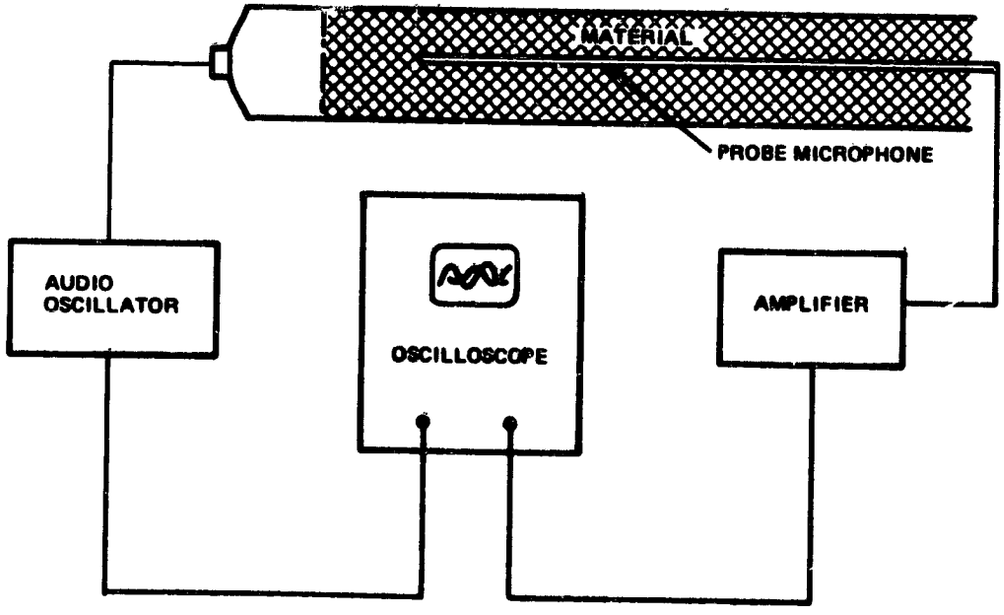

Figure 4. Apparatus for Measurement of Propagation Constant

2.2 NONLINEAR IMPEDANCE OF THIN SHEETS

Up to this point it has been implied that the material impedance is independent of the absolute amplitudes of the acoustic motion; by definition this should be so since the propagation processes are described by acoustic, or linear equations. However, it has been pointed out that the propagation processes are not considered within the material itself, as such; this is avoided by the use of the material impedance concept. It turns out that the fluid motion near and within many lining materials of practical interest, at the sound pressure amplitudes encountered in aero-engine ducts, is not a linear process and hence the impedance concept has to be used with care.

An effective liner impedance needs to be redefined; this is outlined in this section and the necessary types of modification of the linear material impedance parameters are described. It also appears that, although less well documented and understood, the effective liner impedance is also a function of the local grazing mean flow velocity.

When the fluid motion within a lining material is accurately described by linear equations it follows that a single acoustic wave incident on the liner surface will be partly absorbed and partly reflected, the frequency of the reflected wave being the same as that of the incident wave. In addition the impedance seen by the local sound field is independent of the incident wave amplitude. In practice the impedance of most lining materials is dependent on the incident wave amplitude and furthermore the frequencies of the motion are not confined to the frequency of the incident wave. The existence of nonlinear effects is corroborated by the zero frequency or steady flow case where it is well known that the mean pressure differential across a porous material at a sufficiently high Reynolds number is proportional to the square of the steady flow velocity. Based on this zero frequency case it has been postulated by Zorumski and Parrott (Reference 9) that the instantaneous pressure differential $\Delta p(t)$ across a thin porous material is related to the total instantaneous fluid velocity $v(t)$ normal to the sheet by

$$\Delta p(t) = R_t[v(t)]\, v(t) + X_t\, [v(t)] \frac{\partial v}{\partial t} \qquad (7)$$

where $R_t[v]$ is the measured steady flow resistance at the steady flow velocity v, and subscript t emphasizes the dependence on time, t. Since at high Reynolds numbers

$$R_t[v] = b|v| \tag{8}$$

where b is a constant; it follows that (neglecting $X_t[v(t)]$ for the present)

$$\Delta p(t) = b\, v(t)\, |v(t)| \tag{9}$$

Suppose now that only one frequence, ω_1, of fluid motion is present,

$$v(t) = v_1 \sin(t) \tag{10}$$

(here $t = \omega_1 t^*$) then

$$\Delta p(t) = b v_1^2 \sin(t)\, |\sin(t)| \tag{11}$$

or

$$\Delta p(t) = \begin{cases} + b v_1^2 \sin^2(t), \; o \le t \le \pi \\ \\ - b v_1^2 \sin^2(t), \; \pi \le t \le 2\pi \end{cases} \tag{12}$$

Taking the Fourier transform of each side we get, following Zinn (Reference 10) and Melling (Reference 11)

$$\Delta p_1 = \frac{8b}{3\pi} v_1^2 \tag{13}$$

where Δp_1 is the Fourier component of the fluctuating pressure differential at the fundamental frequency ω_1. It follows that the impedance expressed as

a ratio of the pressure differential and the particle velocity at the fundamental frequency is

$$R_1 = \frac{\Delta P_1}{v_1} = \frac{8b\,|v_1|}{3\pi} \quad . \tag{14}$$

At sufficiently low Reynolds numbers R [v] is independent of v

$$R[v] = a \tag{15}$$

and then $R_1 = a$ (16)

In general, both linear and non-linear effects are present so that

$$R_1 \cong a + \frac{8b\,|v_1|}{3\pi} \tag{17}$$

This oversimplified example serves to illustrate two points: (1) that given a particle velocity motion at particular frequency, fluctuating pressures at other frequencies are generated when nonlinear effects are present (given by the Fourier components at higher harmonics of the expression for $\Delta p(t)$) and (2) that an impedance can still be defined in the nonlinear case but it is proportional to the particle velocity amplitude. In general, the particle velocity motion will contain a wide range of frequencies and hence the impedance at one frequency is influenced by motion at all other frequencies. Thus, although the impedance parameter can still be defined in the same way, it will no longer be a function of the material properties alone but is a nonlinear function of the spectral distribution and level of the local sound field (References 9, 12). One other point that is obscured in these introductory notes is that the particle velocity is not known, a priori, rather it is an estimate of the sound pressure level. Thus, an iterative procedure is required in general, although with certain assumptions this can be replaced by the solution to a simple quadratic equation.

2.2.1 Perforated Sheets

A common approximation for the impedance of perforates is

$$\Delta Z_\omega = [a + bv_e] - i[g - hv_e] \tag{18}$$

where v_e is an estimate of the total effective particle velocity normal to the material surface; b and h depend on the material geometry and mean properties of the local fluid but h is also a function of v_e. For all thin porous materials the parameter b can be determined from the steady flow resistance at large velocity v. For perforate materials three similar empirical expressions for b are available, one is given by Mariano (Reference 13) as

$$b = 1.14\left(\frac{1-\sigma^2}{\sigma^{2.1}}\right)\exp\left[-.507\ell^*/d_h^* - 1.7\left(\frac{f\ell^*}{c_a}\right)\frac{\sigma}{v_e}\right] \tag{19}$$

The other expression, given by Rice (Reference 14), is bound up with the definition of the total effective particle velocity which he gives as

$$v_e = \left\{\sum_{i=1}^{N_f} v_{i\ell}^2\right\}^{1/2} \tag{20}$$

$$v_{i\ell} = |v_i| \exp\left\{-[d_h\sigma/|v_i|]^2\right\} \tag{21}$$

and v_i is the effective particle velocity at frequency band i. With those definitions Rice (Reference 14) defines the parameter b as

$$b = \frac{1}{\sigma^2} \tag{22}$$

There is a similarity between the two expressions if we ignore the exponential terms and note that usually $\sigma^2 << 1$; then they differ by a factor $1.14/\sigma^{0.1}$. Also the exponential term in Rice's (Reference 14) expression has an argu-

ment which is of the same form as that in Mariano's (Reference 13) that is, the ratio of a material length scale (hole diameter or sheet thickness) and the particle displacement magnitude ($|v_i^*|/\omega$). Mariano's (Reference 13) expression also contains another exponential term, which is a function of the hole aspect ratio ℓ^*/d_h^*, which is absent from Rice's (Reference 14) expression. The explanation for the former term is given by Rice (Reference 14); he argues that when the fluid displacement is small compared with the hole diameter the "jet will not fully form" and hence the dissipation will decrease. The choice of the hole depth as the significant length scale is seconded by Melling (Reference 11) who has shown that the nonlinear resistance depends on the orifice discharge coefficient which, in turn, depends on the ratio of thickness to hole diameter. The origin of the terms

$$\frac{1}{\sigma^2} \text{ and } \frac{1-\sigma^2}{\sigma^2}$$

in these expressions is, of course, in the well established, steady flow expressions.

A link between these two expressions is found in that given by Armstrong (Reference 15):

$$b = \frac{\pi}{2\sqrt{2}}\, 1.0251 \left(\frac{1-\sigma^2}{\sigma^{2.1}}\right) \exp\left[-.5072\ \ell^*/d^* - 1.8(fd^*\sigma/v_e^*)^2\right] \qquad (23)$$

that is, it is very similar to Mariano's expression except for the exponential term representing the displacement effect which is identical in form to that given by Rice (Reference 14). To summarize, there is clearly agreement that the parameter b should be proportional to the inverse square of the open area ratio but that is all, apart from the consensus that a correction should be applied in the form $\Phi(f\ell^*/v_e^*)$ where ℓ^* is a representative length or effective thickness of the material (Reference 16). More work is needed to establish a generally accepted, precise form for this function and any other corrections which appear to be necessary.

The correction for the nonlinear reactance h is based on experimental observation such as by Ingard and Ising (Reference 18), Zorumski and

Parrott (Reference 9), and Melling (Reference 11), but no formulae appear to be generally available for this effect.

The calculation of the effective particle velocity is, according to some authors, bound up with the grazing flow effects.

2.2.2 Uniform Porous Materials

At high sound pressure levels when nonlinear effects occur Zorumski and Parrott (Reference 9) have verified experimentally that the basic assumption of Equation 7 is correct, that is, the material properties are simply described in the time domain by the measured functions $R_t[v]$ and $X_t[v]$. These functions are the generalizations of the resistance and reactance used to characterize the material in the frequency domain. The spectral impedance Z_ω is not uniquely defined since it will depend on the incident pressure spectrum in a complicated way. For thin porous sheets of material, it is believed adequate to assume $X_t[v(t)]$ is the constant reactance measured in a low intensity test. The resistance $R_t[v(t)]$ can be measured in a flow resistance test since R_t is a function of velocity only.

Assuming a line spectrum where $\Delta p(t)$ and $v(t)$ are given by

$$\begin{Bmatrix} \Delta p(t) \\ v(t) \end{Bmatrix} = \sum_{n=-\infty}^{\infty} \begin{Bmatrix} \Delta p_n \\ v_n \end{Bmatrix} e^{-int} \tag{24}$$

an approximation to the spectral impedance is

$$\Delta Z_n = \frac{1}{2\pi} \int_{-\pi}^{\pi} R_t[\tilde{v}(t)]\, e^{int}\, dt - inX_i \tag{25}$$

where $\tilde{v}(t)$ is an estimated velocity. The velocity estimate may be the result of solving the problem with the assumption that R_t is a constant which is, in turn, estimated.

Very little is known about the dependence of the resistance R_t (which is also the flow resistance) on more fundamental properties of porous

materials. Zwicker and Kosten (Reference 17) and Bies (Reference 6) express the flow resistance in terms of such things as porosity, bulk density, and structure factor, but these variables must be measured so this equation is just pushing the measurement problem from one spot to another. It seems preferable to regard R_t and X_t as fundamental properties of and acoustic material and face the problem of measuring these functions directly.

2.2.3 Measurement Methods

Measurement methods for nonlinear thin sheets are similar to the linear methods for thin sheets except that steps must be taken to account for the higher harmonics of the fundamental frequency which are generated, either by the material nonlinearity or by other nonlinearity in the experimental device such as the acoustic driver in an impedance tube.

Ingard and Ising (Reference 18) measured the impedance of a single orifice at the end of a tube by using a hot wire to measure the velocity in the orifice and a pressure pickup in the side of the tube near the orifices. A crude Fourier analysis of the signals gave the amplitude of the fundamental and the phase of the pressure relative to the velocity.

Melling (Reference 8) has used both the two microphone method and the standing wave method to measure nonlinear impedance of perforates. Narrow band filters were used to eliminate the higher harmonics such that the standard measurements could be made on the fundamental frequency. This approach is not reliable, however, because, even though the filters remove the higher harmonics from the measurement, these harmonics still interact with the fundamental frequency in the material and affect the measurement indirectly. If the acoustic driver is given a distorted signal, or if the tube is operated near a resonant frequency such that shock waves begin to develop, the measured impedance of the material will show these effects even though the signals have been perfectly filtered. Thus, the measured impedance of the material is a function of the entire system properties and has no meaning as a material property at all. The solution to this problem requires a redefinition of the impedance concept and an improved experimental technique.

The new impedance concept required for nonlinear impedance was given by Zorumski and Parrott in Reference 9, and is represented by Equation 7. This impedance concept used a time domain expression for the material property. The acoustic resistance and reactance, as given by Equation 7, depend only on the velocity through the material. An immediate consequence of this assumption is that the acoustic resistance must not depend on the fundamental frequency or the presence of higher harmonics in an impedance tube test. This definition of impedance, if it is correct, is therefore a material property which does not depend on the properties of the measurement apparatus as does the more conventional definition of nonlinear impedance in the frequency domain. Zorumski and Parrott showed that their definition does indeed represent a sample of material over a wide range of test frequencies and intensity levels, from zero frequency, the dc flow resistance, to a 4,000-Hz fundamental frequency test. The measurement method used in this test was the two-microphone method with the backing cavity adjusted to one-fourth of the fundamental test frequency wavelength. The microphone signals were Fourier analyzed and the instantaneous pressure differential, velocity through the sample, and acceleration through the sample were found to determine the resistance and reactance functions in Equation 7.

The preceding discussion shows that the spectral impedance of a nonlinear material depends on the entire frequency spectrum. Wirt (Reference 19) recognized this intuitively and defined impedance as follows: "The impedance at the surface of a nonlinear acoustical material is the ratio of the pressure to the particle velocity, at a particular frequency, and in the presence of a specified sound spectrum and a specified turbulence spectrum." Wirt regarded the effect of flow as causing turbulent pressure fluctuations which would induce a normal velocity through the material. Although he had no convenient way of simulating the flow effect, he did devise a method of measuring impedance, by the standing wave method, in the presence of an intense broadband spectrum. Wirt's impedance tube used three drivers to generate a broadband spectrum of specified shape and intensity, while a fourth driver added a pure tone which was used for the impedance measurement. One-third octave band and 1.8-Hz bandwidth tracking filters, tuned to the oscillator frequency were

used to recover the tone standing wave pattern. Note that if v (t) in Equation 25 in an intense broadband spectrum, Equation 25 represents Wirt's definition of the impedance.

2.2.4 Linearization of Impedance

In this and the previous section the particle velocity normal to the liner surface has appeared in formulae for nonlinear modifications to the liner impedance and the same quantity is also used by Rice (Reference 14) to relate the flow-induced pressure fluctuations to a flow-induced modification to the linear impedance.

This quantity is not known a priori in practical applications nor is it easily measured; the same is true, in fact, for the sound pressure level although it is relatively easy to measure and the existence of nonlinear effects makes it essential, at least, to estimate the sound pressure level at, or near, the liner surface. The relationship between some sound pressure level and the particle velocity is often glossed over in the literature; sometimes the plane wave relation is used (without justification) so that

$$v_\omega^* = p_\omega^* / \rho_a c_a \tag{26}$$

where p_ω^* is the pressure amplitude, but of course the correct relation is

$$v_\omega^* = p_\omega^* / \rho_a c_a Z_\omega \tag{27}$$

(by definition). Two problems immediately arise: the pressure p_ω^* is the complex amplitude actually at the lined surface and is, itself, a function of v_ω^*. It is not the pressure amplitude in a hard-walled duct and in principle it is not known until it can actually be measured with the liner installed. A further complication is that the particle velocity, it is argued, at one particular frequency should be replaced by a total effective particle velocity when using the nonlinear impedance modification formulae, since the nonlinear bias is a response to the particle velocity at all frequencies. Thus, Rice (Reference 14) and others have defined the total effective particle velocity to be

$$v_e^* = \left[\sum_{i=1}^{N_f} \left| v_i^* \right|^2 \right]^{1/2} \tag{20}$$

where

$$v_i^* = \frac{p_i^*}{\left| \rho_a c_a Z_i \right|} \tag{29}$$

(the i subscript denotes a frequency or frequency band and the summation is over all the frequency bands which may contribute a significant value for p^*_i). In this case p^*_i the pressure amplitude in frequency band i is assumed known. Note, however, that $Z_i \equiv Z_\omega$ is calculated using expressions of the form

$$Z_\omega = \left[a + b \left| v_e \right| \right] - i\left[g - h \left| v_e \right| \right] + i \cot(k^* d^*) \tag{30}$$

Then v^*_i and hence v^*_e is calculated using the previous two equations which completes the first loop; with the new value of v_e the impedance Z_ω can be recalculated and the iteration repeated until two successive values of Z_ω are nearly the same.

In principle, of course, the pressures p^*_i are not known and incorrect trends may be obtained from assuming that p^*_i is a constant in these iterations. It is preferable, following Ingard, (Reference 18) to work in terms of an incident sound pressure amplitude, p^*_i, and then the particle velocity v^*_i is given by

$$\left| v_i^* \right| = \frac{2p_{0i}^*}{\rho_a c_a \left| Z_i + 1 \right|} \tag{31}$$

Twice the incident pressure amplitude, $2p^*_{0i}$, can be loosely identified with the pressure amplitude in frequency band i in a given duct system when the duct walls are unlined.

2.3 THE EFFECT OF GRAZING FLOW

2.3.1 Empirical Models

There is at least one physical effect of sheared mean flow on sound propagation and attenuation in lined flow ducts which is well established in that it has been extensively studied, at least analytically. Physically it is the refraction and convection of sound by the mean flow. This effect, when included in the propagation equations, yields calculated values for, say, the modal attenuation rates which do not appear to agree with experiment (Kurze and Allen, Reference 20), unless a modification is assumed for the liner impedance. In addition, from certain experiments, measured liner impedances in the presence of grazing flow confirm that a modification appears to take place although all experiments to date have been questioned in certain respects. While measured attenuation rates do strongly indicate some sort of modification this may be an incorrect interpretation insofar as there may be other physical effects which are not accurately represented in the propagation equations. However, for the present, this semiempirical effect is accepted and expressed as a modification in the form of an additional term, to the zero-flow impedance. Incidentally, there is no a priori reason why an additive term for the impedance is appropriate. It could be equally well that an additional term for the liner admittance is appropriate as, for example, in the case where viscous effects on duct propagation are represented in the form of an additional admittance (Reference 21).

Kurze and Allen (Reference 20) state that "the reactive component of a lining with perforated plate has to be reduced and the resistance had to be chosen higher than the liner acoustic resistance of the particular material" to obtain good agreement between experimental and theoretical attenuation rates. They "assume that the resistance of a nonlinear material increases with sound-pressure difference across the lining" but that "the observed proportionality factor between the nonlinear influences of flow and sound is higher than expected from turbulent pressure fluctuation at a smooth hard wall . . . . The (measured level) is at least 10-15 db lower (however) than the equivalent level . . . (but) recent data show that the roughness of a wall can substantially increase the wall pressure fluctuations." They

conclude that further investigations are required in this subject and that the effective resistance should be proportional to the Mach number of the mean flow.

The idea that the turbulent boundary layer may interact with a porous wall, in particular a perforate lining, to give rise to the implied effects has been developed in at least three ways.

First, Rice (Reference 14) has argued that the unsteady jets issuing from each hole interact with the grazing flow: "pressure oscillations are produced within the potential core of the jet due to vortex shedding from the grazing flow over this core." Rice deduces an expression for the maximum value of pressure fluctuations, $p^*_{g,\,max}$, which is of the form

$$p^*_{g,\,max} \propto \rho_a U^{*2} \left(\frac{d^*_h}{\delta^*}\right)^2$$

where δ^* is the linear boundary layer thickness. He then shows, with certain assumptions, that through the nonlinear effect outlined in the previous section the value of the resistance under a typical grazing flow velocity, U*, will be

$$R^*_\omega \propto \left(\frac{U^* d^*_h}{\delta^*}\right) \frac{1}{\sigma}$$

This linear dependence on the grazing flow mean velocity is in good qualitative agreement with the direct measurements by, for example, Feder and Dean (Reference 22). Rice (Reference 14) agrees with Kurze and Allen (Reference 20) that the smooth, hard wall, measured pressure fluctuations are too small to explain the grazing flow effect and measurement of pressure fluctuations over lined duct surfaces are urgently required in sufficient detail to checkout his proposed model. An identical grazing flow dependence is deduced by Eversman (Reference 16) by simply assuming that the grazing flow dynamic pressure, p^*_g is given by

$$p^*_g = K \frac{1}{2} \rho_a U^{*2}$$

where K is a function of the grazing flow boundary layer, face sheet surface geometry, and roughness, and is determined empirically.

The second approach is that developed by Ronneberger (Reference 23) originally for the case where the hole diameter is larger than the boundary layer thickness. Based on the concept that the whole boundary layer fluctuates in and out of the orifice and on information concerning the instability of this motion, Ronneberger deduces that the real part of the orifice impedance is proportional to the grazing flow velocity, which is borne out very clearly by his measurements. The dependence on boundary layer thickness is not deduced in detail from his theoretical model, but he argues that it is of the same form as that deduced by Rice (Reference 14), if $\delta^*/d_h^* \ll 1$ and $\omega\delta^*/U^* \ll 1$. It should be emphasized that Ronneberger's work is mainly concerned with the case $\delta^*/d_h^* \ll 1$ and that his postulated mechanism differs from that of Rice (Reference 14) in that the latter author appeals to the nonlinear response of the perforate whereas Ronneberger views the effect as a flow induced change in the radiation impedance of a single orifice.

Another mechanism has been proposed by Hirata and Itow (Reference 24) based on the argument that the kinetic energy of the motion in the vicinity of the orifice is "carried away" by the airstream and thus since energy "dissipation depends on the diffusion of energy from the resonator into the surrounding medium" the dissipation (by the orifice) depends on the (grazing) airflow. They develop simple equations to describe these energy related concepts and deduce the same dependence on airflow velocity as the previous authors mentioned above. They use their formula for the flow-induced resistance in transmission loss calculations which they compare with measurements for mean-flow velocities up to 50 m/s and find reasonable qualitative agreement.

Another feature of the flow induced change in acoustic material properties is given by Budoff and Zorumski in Reference 25. When there is a tangential flow on a side of a thin sheet, it cannot be assumed that the resistance, R, for blowing into the stream is the same as for sucking from the stream. The flow resistance of perforated sheets was therefore measured with both

blowing and sucking and the results were compared. It was found that there was an added resistance which is proportional to tangential velocity, as in the previous discussion, but that the factor of proportionality was not the same for blowing as it was for sucking. These results, illustrated in Figure 5, were not explained and are in need of independent confirmation.

CR48

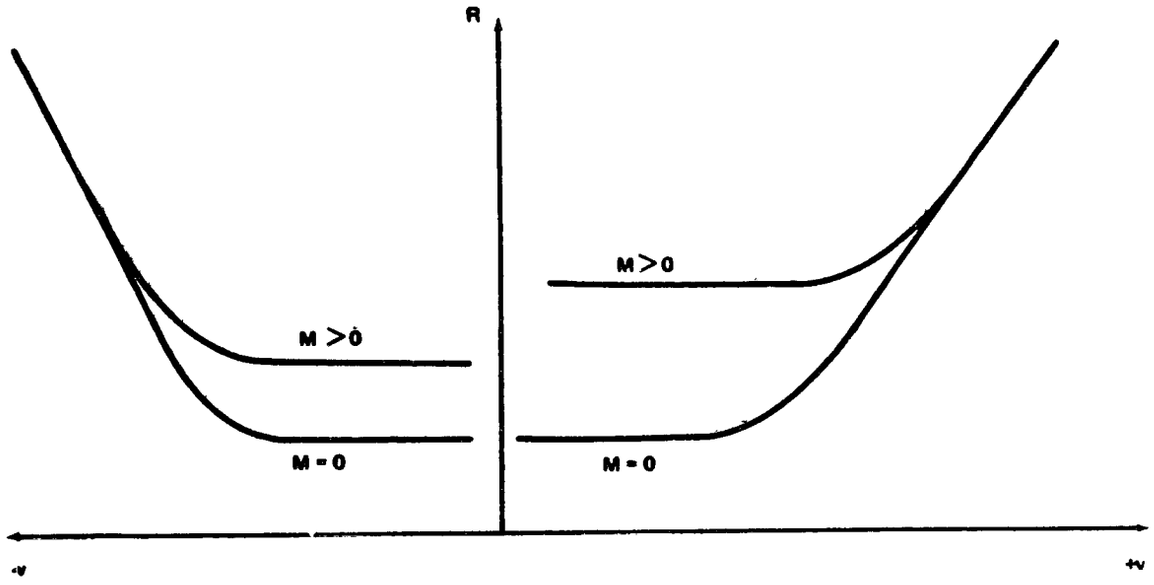

Figure 5. Dependence of Flow Resistance of Perforated Sheet on Tangential Mach No. M ($=U^*/c_0$) and Normal Mach No., v. Negative v Indicates Boundary Layer Blowing and Positive v Indicates Suction

Experiments with a single orifice in the presence of grazing flow (Reference 22), however, still show a close correlation between acoustic resistance and flow resistance. This correlation can be explained from the study by Posey and Compton (Reference 26) which shows an equivalent resistance can be defined in terms of the resistances for blowing and sucking. This equivalent resistance is a weak function of the difference in the actual resistances and is roughly $2R_+R_-/(R_+ + R_-)$, where R_+ is the resistance for sucking and R_- is the resistance for blowing.

Some unpublished measurements were made by Feder (Pratt & Whitney Aircraft, East Hartford, CN) of the flow resistance of perforated sheets in the presence of tangential flow. Feder's data were subsequently correlated

by Rogers and Hersh (Reference 27) in terms of a discharge coefficient, C_D which is related to the specific orifice resistance by

$$R_h = \frac{|v|}{2\sigma C_D^2} \tag{32}$$

For a sample with $\sigma = 0.141$, the resulting resistances become

$$R_+ = \frac{(v_+)^{0.06} M^{0.94}}{0.63} \tag{33}$$

and

$$R_- = \frac{(v_-)^{-0.30} M^{1.30}}{5.4} \tag{34}$$

with similar results for other specimens. These results exhibit a discontinuity at the point of flow reversal between blowing and sucking because of the singularity in expression for the resistance with blowing R_-, but that is consistent with the measured results of Budoff and Zorumski (Reference 25).

It is quite clear from these and other publications that this flow induced effect, whatever its physical interpretation, is extremely important in flow duct liner design for all practical liner materials, but particularly for locally reacting perforate materials, and it is also the least understood.

2.3.2 Measurement Methods

A number of methods have been attempted to measure the impedance of an acoustic material or an orifice with grazing flow. Before discussing these, however, we will briefly mention the far simpler measurement of flow resistance used by Budoff and Zorumski in Reference 25. The experimental setup is shown in Figures 6 and 7. The essential part of the method is the measurement of the differential in static pressures between the flow duct and the side branch and the measurement of steady velocity through the sample. Since the pressure differentials may be quite small, it is necessary to have a sensor which will indicate differentials down to 10^{-5} atmospheres and up to 10^{-2} atmospheres.

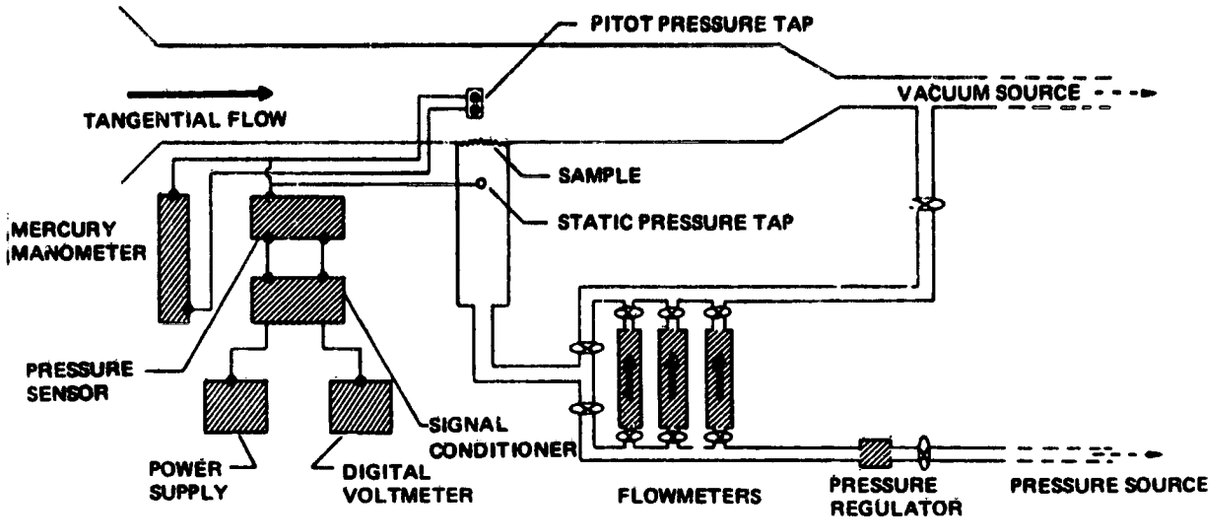

Figure 6. Schematic Drawing of Apparatus

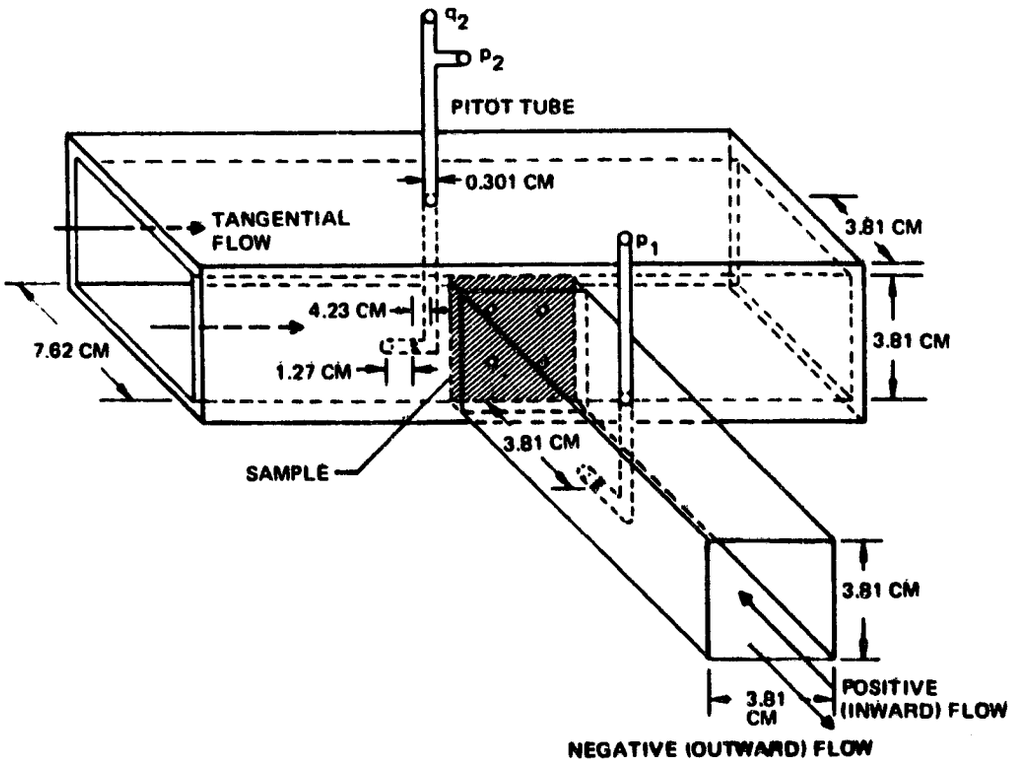

Figure 7. Test Section (40 cm from Tangential-Flow Intake to Sample)

A similar large range of flow rate is required. This was accomplished by using three rotameter flow meters with a suitable pipe and valve arrangement as shown on Figure 6. This system also utilizes the same flow meter for both blowing and sucking flow rates, so that any asymmetry observed in the resistance cannot be due to switching flow meters.

Feder and Dean (Reference 22) measured the impedance of thin sheets in the presence of grazing flow using the standing wave method. The sample was mounted in the side of a small flow duct, as in Figure 6, and the side branch was used as an impedance tube. The principal difficulties of this method were accurate measurement of the standing wave pattern and uncertainty about the radiation impedance of the tube, looking into the flow duct.

Ronneberger (Reference 23) used an apparatus similar to Ingard and Ising's (Reference 18) to measure the radiation impedance of an orifice looking into a shear flow. Some of his results have been discussed previously in this report. We note here, however, that Ronneberger found that the acoustic resistance and flow resistance of the orifice were nearly identical and that the reactance decreased with increasing tangential flow.

Armstrong, Beckmeyer, and Olsen (Reference 28) measured the impedance of a wave in a flow duct with one treated wall by measuring the axial wavelength and decay rate of a duct mode with a two-microphone technique. The apparatus is shown in Figure 8. In this method, the shear flow profile is measured and the shear flow wave equation is solved to relate the duct liner impedance to the measured axial wave number. The advantage of this method is that it tests a complete duct liner under conditions simulating its intended application. Its disadvantages are that it requires large material samples and an elaborate data reduction scheme. (Also, it does not appear to be easily extended to the measurement of nonlinear impedance.)

Dean (Reference 29) used a one-microphone method (not previously discussed here) and the two-microphone method to measure the impedance of duct liners in the presence of flow. Dean's results indicated that the two-microphone technique was preferable. This method has the advantage of being applied to a finished duct liner, like Armstrong's method, and has the added advantage of being able to measure nonlinear impedance.

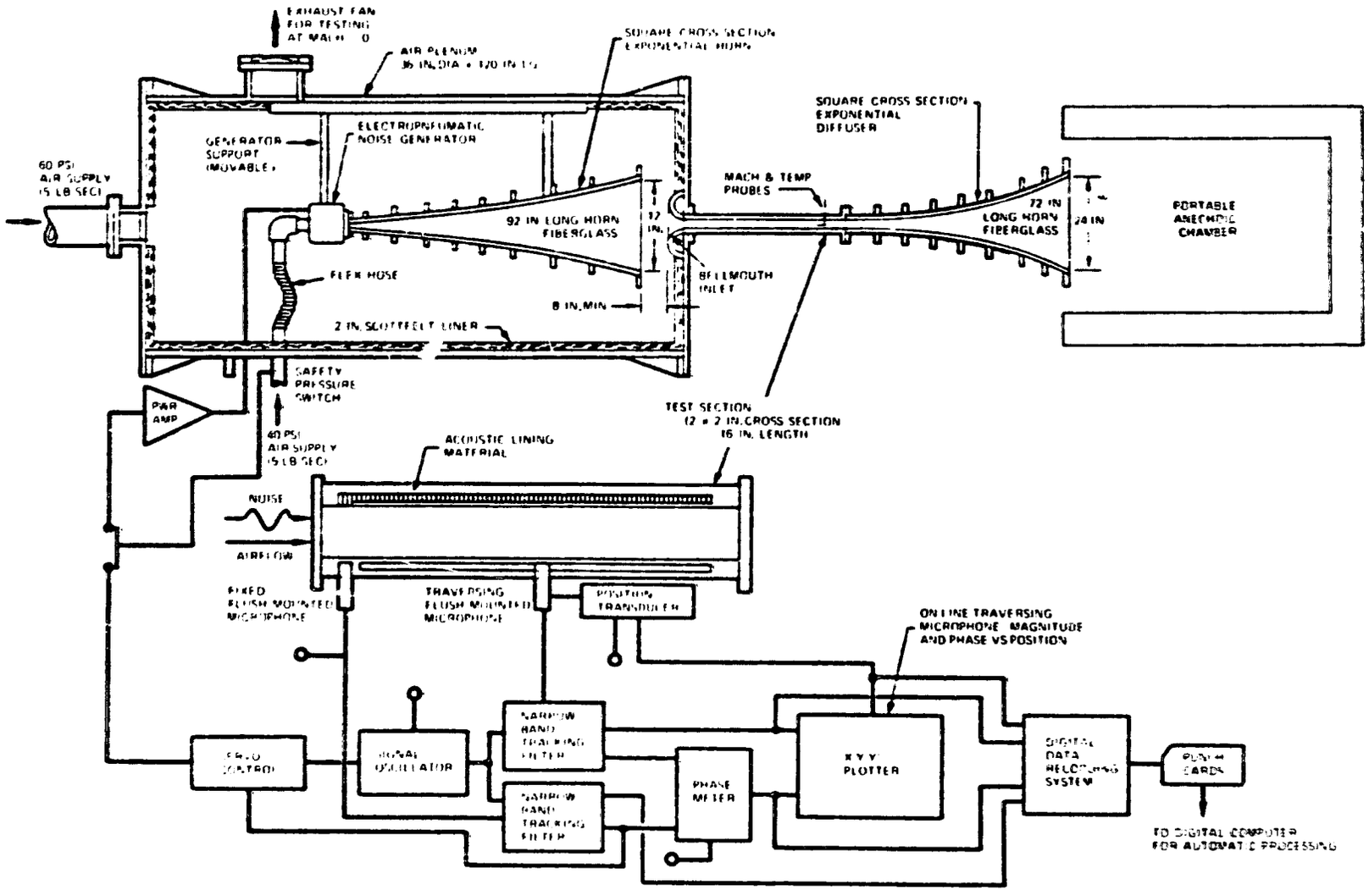

Figure 8. Grazing Flow Apparatus Instrumentation

2.4 RECOMMENDED METHODS FOR MATERIALS

Bulk materials are not often used in aircraft engine duct applications, however, their use is always a possibility so that they should be included in any prediction scheme. Little is known about nonlinear behavior of bulk materials. The work mentioned here has been concerned with linear properties. This linear representation may be acceptable in the aircraft engine application because a bulk material in a duct liner would probably be protected by a facing sheet which would cut down on the amplitude of the waves in the material. For prediction purposes, therefore, it is recommended that:

Bulk materials are assumed to be linear and described through the equations

$$\vec{\nabla} p_\omega + z_\omega v_\omega = 0 \tag{35}$$

and

$$\nabla^2 p_\omega + k_\omega{}^2 p_\omega = 0 \tag{36}$$

where z_ω and k_ω are experimentally measured complex material parameters which are functions of frequency.

Sheet materials which are essentially rigid, both perforated sheets and uniform porous materials, are typically used in aircraft engine as facing sheets which are exposed to high intensity sound and to grazing flow. It has been demonstrated many times that there is a close correspondence between measured acoustic resistance (in the frequency domain) and flow resistance. Also, time domain measurements have shown this equivalence between flow resistance and instantaneous resistance for intense waves with fundamental frequencies up to 4,000 Hz. Therefore there is no question that the quasi-static assumption is valid over the entire range for which measurements can be accurately made. Less is known about the reactive part of the material impedance. This term is always small compared to the resistive part at high amplitudes so that it is extremely difficult to measure; however, since it is not a dominant effect there is little motivation to measure it and, as an approximation, it may be assumed to be indedendent of level, that is, the reactive part of the material impedance is linear.

It is known that grazing flow affects the resistive part of the impedance of a thin sheet. The effects seems to be directly proportional to grazing flow velocity (in the free stream) and inversely proportional to boundary layer thickness. It also seems that the proportionality constants of the flow resistance are slightly different for boundary layer blowing than they are for boundary layer suction. This difference implies that there is a peculiar sort of nonlinearity induced by the grazing flow, even at low sound pressure levels.

The following expression is recommended to represent the acoustic properties of all thin sheet materials:

$$\Delta p^* = Z_t v^* \tag{37}$$

where

$$Z_t^* = \rho_a c_a \left\{ R\left[v,\ M,\ \left(\frac{\delta_1^* c_a}{\nu} \right) \right] + \sigma \frac{\rho_e^*}{\rho_a} \frac{\ell^*}{c_a} \frac{\partial}{\partial t^*} \right\} \tag{38}$$

The nonlinear resistance R is to be measured in a steady flow resistance test. The normal velocity v^* will have the range $10^{-4} \leq |v^*/c_a| \leq 10^{-2}$ in both the blowing ($v^*/c_a < 0, M > 0$) and suction ($v^*/c_a > 0,\ M > 0$) measurements. The free stream Mach number shall have the range $0 < M < 0.5$ and the boundary layer displacement thickness shall be chosen to correspond to the intended applications of the data. The measured data are to be correlated in terms of a discharge coefficient, in terms of which R is given as

$$R = \frac{|v|}{2\sigma^2 C_D^2} \tag{39}$$

and the discharge coefficient shall be asymptotic to $\sqrt{|v|/M}$ if $|v| \ll M$ and to a constant when $|v|$ is of the same order as M. In addition, R is taken to approach a constant when both M and $|v|$ are small. The reactive part of the impedance, X_e, may be measured at a low intensity ($100 \text{ db} \leq L_p \leq 120 \text{ dB}$) by either the standing wave or the two microphone

method, with the material placed in front of a quarter-wave backing cavity. The impedance is to be linearized by computing an effective velocity

$$v_e = \left\{ \sum_{i=1}^{N_f} |v_i|^2 \right\}^{1/2} \tag{40}$$

$$R_e = \frac{2\, R[+ v_e]\; R[-v_e]}{R[+v_e] + R[-v_e]} \tag{41}$$

so that the material impedance is

$$\Delta Z_\omega = R_e - i\sigma \rho_e \ell \tag{42a}$$

or

$$\Delta Z_\omega = R_e - iX_e \tag{42b}$$

If X_e is measured at only one frequency, the expression in Equation 42a can be used to calculate ΔZ_ω at any other frequency by assuming σ, ρe and ℓ^* are frequency independent (note $\ell = \omega \ell^* / c_a$). However, it is preferable to take measurements of X_e at all frequencies of interest and then to use Equation 42b.

Section 3
DUCT LINERS

3.1 FLAT POINT REACTING LINERS

Under certain conditions the impedance normal to and at the lined surface is a function of only the liner parameters, except for certain local mean flow properties such as the mean density and the coefficient of viscosity. In particular, when it is independent of the properties of the local sound field (apart from its frequency) the lined surface is said to be point reacting. Physically, the simplest feature of point reaction is that the direction of acoustic motion within the liner is independent of the direction of an incident plane wave.

The impedance normal to and at the surface of a flat, point reacting single-layer configuration (backed by an impervious, rigid wall) is of the form.

$$Z_\omega = \Delta Z_\omega + i\, k_a/k^* \cot(k^* d^*) \tag{43}$$

The second term is the impedance of the air-cavity under these conditions where d^* is the cavity depth and k^* is the wave number of the motion in that cavity. In most applications it has been assumed that this motion is in the form of a plane wave so that $k^* = k_a = \omega/c_a$. Melling (Reference 11) has noted that, due to viscous and other dissipative effects on propagation within the honeycomb cavity it is preferable to assign a small imaginary part to this wave number, which could be obtained from impedance tube or in situ measurements. If only viscous effects are taken into account then (Reference 11) k^* is given by

$$k^* = \frac{\omega}{c_a} + \frac{i}{r_e^* c_a}\left(\frac{\omega\nu}{2}\right)^{1/2} \tag{44}$$

where r_e^* is the effective radius of the honeycomb cell and ν is the kinematic viscosity of the cavity fluid. The general form of the air-cavity impedance expression is for the case when the cavity walls are normal to the porous sheet surface. Appropriate modifications are needed if the cavity has a variable cross-sectional area and/or the walls are not normal to the porous sheet. Developments in this direction are being pursued by Wirt (Reference 30) for complicated but point reacting liner configurations which have desirable features such as good low frequency absorption relative to standard configurations of the same depth, and wide-band absorption characteristics previously thought unattainable with their porous material cavity combination.

The locally reacting liner may be of the multilayer type, that is, made up of a number of porous sheets separated by honeycomb layers of various depths. For simplicity we consider the flat single layer type although, in principle, the information summarized here can be applied to convex and concave, multilayer, locally reacting configurations; general expressions for the impedance of those configurations are given by Zorumski (Reference 31) in terms of the linear impedance of each material layer and the distances between or depths of each layer. Following the analysis of Zwicker and Kosten (Reference 17), it can be shown that the impedances of successive layers of a duct liner are related by the recurrence formula

$$\begin{Bmatrix} p_\omega \\ v_\omega \end{Bmatrix}^{(n)} = \begin{bmatrix} 1 & \Delta Z_\omega \\ 0 & 1 \end{bmatrix}^{(n)} \begin{bmatrix} \cos k_\omega d & \frac{z_\omega}{k_\omega} \sin k_\omega d \\ \frac{-k_\omega}{z_\omega} \sin k_\omega d & \cos k_\omega d \end{bmatrix}^{(n)} \begin{Bmatrix} p_\omega \\ v_\omega \end{Bmatrix}^{(n-1)} \qquad (45)$$

where

$$z_\omega^{(n)} = -i, \; k_\omega^{(n)} = 1$$

if the medium within the honeycomb cavities is at ambient conditions.

3.2 FLAT EXTENDED REACTION LINERS

In general, the liner impedance concept is most useful when the liner is of the point reacting type. At the other extreme when the normal impedance at the lined surface is, say, a function of the angle of incidence but still independent of position, the impedance concept can still be used to some advantage, as outlined below. However, in order to incorporate the more realistic case when the impedance is a function of position, the impedance concept, per se, can be discarded in most extended reaction cases in favor of a different approach. That is, sound propagation through the liner itself is included in the description of the wave propagation throughout the duct. The boundary condition for the wave propagation process is still in the form of an impedance or admittance parameter, but the surface at which it is applied is elsewhere such that point reaction can still be assumed.

An extended reaction liner is one in which there may be waves propagating parallel to the duct axis, circumferentially around the duct perimeter, or in both directions. It is assumed here that the liner is made up of N uniform, layers of bulk-type porous material and thin sheets of rigid material such as perforated plates. This liner construction is shown in Figure 9.

CR48

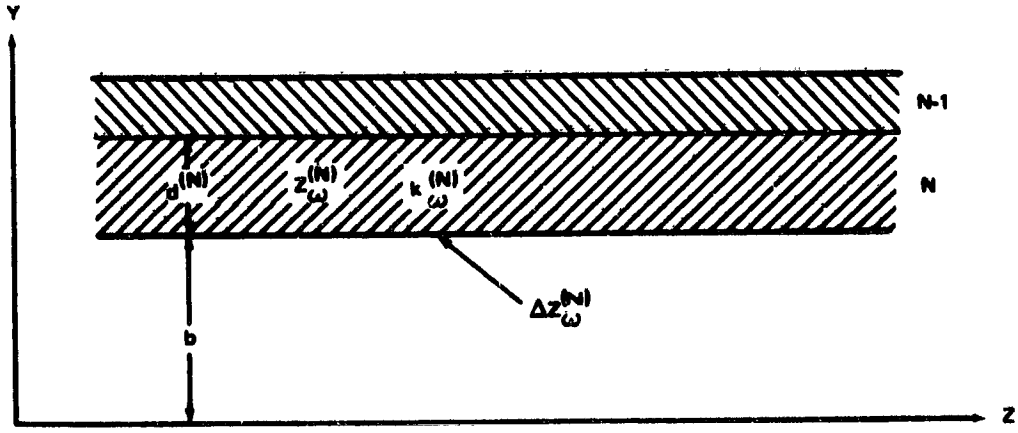

Figure 9. Duct with Multilayered Nonlocally-Reacting Liner.

When duct liners are sufficiently thin for curvature effects to be neglected, their analysis may be carried out in rectangular coordinates. In this case, the wave numbers are related by

$$(k_{rm}^{(n)})^2 = (k_{\omega}^{(n)})^2 - (k_{zm})^2 - (m/b)^2 \qquad (46)$$

Following the analysis by Zwicker and Kosten (Reference 17), it can be shown that the pressures and velocities of successive layers of the duct liner are related by the recurrence formula (Equation 45) if $k_{rm}^{(n)}$ is substituted for $k_{\omega}^{(n)}$. If the liner is partitioned so that waves may not travel axially, k_{zm} is set to zero, and if they may not travel circumferentially, m is set to zero. Thus, Equation 45 provides a means of calculating the surface impedance of uniform, multi-layered extended reaction liners.

Through Equation 46 the surface impedance of such a duct liner may be a function of the circumferential and/or axial wave numbers. This generally presents no difficulty as far as the circumferential wave number is concerned, since the acoustic equations in axisymmetric ducts may be solved separately for each circumferential wave. However, the impedance Equation 45 must be evaluated simultaneously with the appropriate duct propagation equations and k_{zm} will be variable during the solution process.

3.3 RECOMMENDED METHODS FOR LINERS

An iteration process must be used to compute liner properties since the impedance depends on the acoustic spectrum through Equation 40. Here we assume that a one-third octave band spectrum of p_{ω} is known at the linear surface. The first step is to compute the resistances of the material layers from some estimate of the corresponding velocities. This information is then used to re-estimate the velocities. The process may be started by assuming all velocities are small so that the material impedances or resistances are independent of velocity. Thus, for a liner with N layers, we start with the velocity vector for each frequency or frequency band i

$$\left\{v_i^{(n)}\right\} = \begin{Bmatrix} v_i^{(N)} \\ v_i^{(N-1)} \\ \cdot \\ \cdot \\ \cdot \\ v_i^{(1)} \end{Bmatrix} = \begin{Bmatrix} 10^{-4} \\ 10^{-4} \\ \cdot \\ \cdot \\ \cdot \\ 10^{-4} \end{Bmatrix} \tag{47}$$

Then Equation 40 is used to compute an effective velocity for each layer

$$\left\{v_e^{(n)}\right\} = \left\{\left[\sum_{i=1}^{N_f} \left| v_i^{(n)} \right|^2\right]^{1/2}\right\} \tag{48}$$

and Equations 41 and 42 are used to compute an impedance vector, $\left\{Z_i^{(n)}\right\}$, at each frequency, where

$$\left\{\Delta Z_i^{(n)}\right\} = \left\{R_e^{(n)} - i\,\sigma^{(n)}\,\rho_e^{(n)}\,\ell^{(n)}\right\} \tag{49}$$

The condition $p_i^{(N)} = p_i$ and $v_i^{(O)} = 0$ are used with sets of Equations 45 to give

$$\begin{bmatrix} \begin{bmatrix} 1 & 0 \\ [I] \end{bmatrix} & \begin{bmatrix} T^N_{N-1} \end{bmatrix} & & \\ & \cdot \cdot \cdot & & \\ & & [I] & \begin{bmatrix} T^2_1 \end{bmatrix} \\ & & & [0 \quad 1] \end{bmatrix} \begin{Bmatrix} p_i^{(N)} \\ v_i^{(N)} \\ \cdot \\ \cdot \\ \cdot \\ p_i^{(O)} \\ v_i^{(O)} \end{Bmatrix} = \begin{Bmatrix} p_i \\ 0 \\ \cdot \\ \cdot \\ \\ \\ 0 \end{Bmatrix} \tag{50}$$

where the identity matrices in Equation 50 are order (2 x 2) and the square matrices (T^n_{n-1}) are the products shown in Equation 45. The solution to Equation 50 at each frequency gives a new set of velocity vectors which may be used to repeat the iteration starting with Equation 47. The iteration

stops when the effective velocity vector ceases to change by a significant amount with successive iterations (or, alternatively, the resistance vector as described in Section 4).

3.4 EXAMPLE LINER

Reference 32 describes the inlet liner for a typical ground test nacelle. The liner is a perforated plate, 0.5-mm thick, with 1.27-mm diameter holes spaced to achieve an open area $\sigma = 0.068$. The backing is honeycomb with a 12.2-mm depth. The needed flow resistance and effective density function for the plate is not known, however they may be estimated. For flow into the liner the orifice discharge coefficient is assumed to be $0.8\sqrt{v/M}$ (Reference 27) and for outflow it is taken as $\sqrt{|v|/M}$. The corresponding orifice resistances are $M/1.28$ and $M/2.0$ and the acoustic resistances (based on average velocity through the plate) are $R_+ = M/0.087$ for inflow and $R_- = M/0.136$ for outflow. The effective density is taken to be the air density so that $\rho_e = 1$. The inlet mach number is 0.58 so that the effective resistance is $R_r = 5.20$. The reactance in Equation 42 is negligible so that Equation 43 gives an impedance of

$$Z_\omega = 5.20 + i \cot (2.253 \times 10^{-4} f),$$

which is $5.20 + i\,4.36$ at $f = 1$ kHz.

Section 4
RECOMMENDED PREDICTION METHODS

4.1 SINGLE-LAYER LINER CONFIGURATIONS

The calculation method falls into two parts. The first is concerned with the cavity impedance, which is assumed to be independent of sound pressure level and grazing flow effects. The second involves an iteration for the sheet material acoustic resistance which is dependent on those effects and which also utilizes the calculated cavity impedance. Input data for both calculations is summarized first, under the data base heading.

It should be noted that symbols like Z_i, p_{io} and v_i have been replaced by $Z(f_j)$, $p_o(f_j)$ and $v(f_j)$; that is, v_i, for example, at frequency band i is now particle velocity $v(f_j)$ at the frequency band j for which the center frequency is f_j. This not only serves to provide an explicit reference to f_j (and prevents confusion between $i = \sqrt{-1}$ and the frequency number), but it distinguishes the parameters used here from their counterparts elsewhere in the report which are often single frequency or spectral (Fourier) quantities. Also is should be noted that, in general, the cotangent function in what follows and the parameters $k^*(f_j)$, $z^*(f_j)$, $Z_c(f_j)$, k_{zm}; k^*_{rm}, $\Delta Z(f_j)$ and $v(f_j)$ are <u>complex</u> quantities.

<u>Data Base</u>

1. Center-band frequencies f_j, $j = 1, 2 \ldots N_f$, Hz
2. Speed of sound in duct medium, c_a, m/sec
3. Characteristic impedance of duct medium, $\rho_a c_a$, MKS RAYLS
4. Sound pressure level spectrum in hard-walled duct, $SPL_H(f_j)$, db re: $p_{ref} = 2 \times 10^{-5}$ N/m^2
5. Incident (normalized) sound pressure spectrum:

$$p_o(f_j) = \left(\frac{\sqrt{2}}{2}\right) \left\{10^{SPL_H(f_j)/20}\right\} \times p_{ref} / \rho_a c_a^2$$

with $SPL_H(f_j)$ from (4), $\rho_a c_a^2$ from (2), (3)

6. R versus v material D. C. flow characteristic (at the required tangential Mach number)
7. Material specific acoustic reactance at each frequency, $X_c(f_j)$
8. Wave number and distributed impedance of cavity filler (if any) at each frequency, $k^*(f_j)$, rad/m and $z^*(f_j)$, MKS RAYLS/m
9. Cavity depth, d^*, m if simple cavity configuration (see (12) below).
10. Honeycomb effective radius, r_e^*, m if simple, small-radius honeycomb forms air-filled[†] cavity.
11. Kinematic viscosity of cavity medium, ν, m^2/sec if simple, small-radius honeycomb forms air-filled[†] cavity.

Calculation of Cavity Impedance

12. The specific acoustic cavity impedance, $Z_c(f_j)$, is determined at each frequency with one of the methods outlined below, as appropriate.

a. Simple air-filled cavity:

$$Z_c(f_j) = i\left\{k_a/k^*(f_j)\right\} \cot\left\{k^*(f_j)d^*\right\}$$

where

$$k^*(f_j) = k_a = 2\pi f_j/c_a$$

or for a "small radius" honeycomb cavity

$$k^*(f_j) = \frac{2\pi f_j}{c_a} + i\,\frac{(\pi f_j \nu)^{1/2}}{r_e^*\, c_a}$$

b. Simple cavity, filled with bulk material:

$$Z_c(f_j) = -z^*(f_j)/\left\{\rho_a c_a\, k^*(f_j)\right\} \cot\left\{k^*(f_j)d^*\right\}$$

c. Complex, point reacting cavity geometries, curved liner configurations, etc. — use measured values for $Z_c(f_j)$ or values calculated according to referenced theoretical models.

[†] i. e., the cavity medium is acoustically identical to the duct medium.

d. Extended reaction (nonpartitioned) liner configurations — the impedance calculation method must be carried out in conjunction with the solution of the duct propagation equation, which provides values for k_{zm} and m/b. In this case $Z_c(f_j)$ is calculated with

$$Z_c(f_j) = \left[-z^*(f_j) / \left\{\rho_a c_a\, k^*_{rm}\,(f_j)\right\}\right] \cot\left\{k^*_{rm}\,(f_j)\, d^*\right\}$$

where

$$k^*_{rm}\,(f_j)/k_a \equiv k_{rm}(f_j)$$

$$= \left\{(k^*\,(f_j)/k_a)^2 - \delta_z\, k^2_{zm}\,(f_j) - \delta_m (m/b)^2\right\}^{1/2}$$

$$(k_a = 2\pi f_j / c_a)$$

and δ_z, δ_m are unity in the absence of partitioning, but $\delta_z = 0$ if the liner is axially partitioned or $\delta_m = 0$ if circumferentially partitioned.

Liner Impedance Calculation: Iteration for Sheet Material Acoustic Resistance

13. Choose an initial value for the sheet material specific acoustic resistance, e.g.,

$$R_e = 1.0$$

14. Form a value for the complex material specific acoustic impedance at each frequency

$$\Delta Z(f_j) = R_e - i\, X_e(f_j)$$

with R_e from (13) or (18) and $X_e(f_j)$ from (7).

15. Form a value for the complex liner specific acoustic impedance at each frequency

$$Z(f_j) = \Delta Z(f_j) + Z_c(f_j)$$

with $\Delta Z(f_j)$ from (14) and $Z_c(f_j)$ from (12).

16. Calculate the complex effective particle velocity Mach number at each frequency

$$v(f_j) = 2p_o(f_j) / \left| Z(f_j) + 1 \right|$$

with $p_o(f_j)$ from (5) and $Z(f_j)$ from (15).

17. Calculate the total effective particle velocity Mach number

$$v_e = \left[\sum_{j=1}^{N_f} \left| v(f_j) \right|^2 \right]^{1/2}$$

with $v(f_j)$ from (16).

18. Read off from $R[v]$, the material D.C. flow characteristic (from (6)), the values R_+, R_- where

$$R_+ = R\left[+v_e\right]$$

$$R_- = R\left[-v_e\right]$$

and calculate the effective specific acoustic resistance

$$R_e = 2R_+R_-/(R_+ + R_-).$$

If this value of R_e differs from its previous value (or if it differs from that assigned in (13) by less than a specified tolerance then the iteration can be terminated and the required specific acoustic liner impedance is the last

value calculated at (15). Otherwise the procedure must be repeated starting at (14) with the new value of R_e or one based upon this and previous values (for example by linear extrapolation).

4.2 MULTILAYER LINER CONFIGURATIONS

The calculation method falls into two parts. The first is concerned with the cavity impedance matrices, which are assumed to be independent of sound pressure level and grazing flow effects. The second involves an iteration for the sheet material resistances which are dependent on the former effect, while the surface layer alone is influenced by grazing flow effects. Input data for both calculations is summarized first, under the data base heading.

The reader is referred to the comments on notation, etc., in the introduction to Section 4.1.

Data Base

1. Center-band frequencies f_j, $j = 1, N_f$, Hz.
2. Speed of sound in duct medium, c_a, m/sec.
3. Characteristic impedance of duct medium, $\rho_a c_a$, MKS RAYLS.
4. Sound pressure level spectrum in hard-walled duct $SPL_H(f_j)$, db re: $p_{ref} = 2 \times 10^{-5}$ N/m^2.
5. Incident (normalized) sound pressure spectrum:

$$p_o(f_j) = \left(\frac{\sqrt{2}}{2}\right)\left\{10^{SPL_H(f_j)/20}\right\} \times p_{ref}/\rho_a c_a^2$$

with $SPL_H(f_j)$ from (4), $\rho_a c_a^2$ from (2), (3).

6. a. The number of material layers, N
   b. $R^{(n)}$ versus v material D. C. flow characteristic for each material layer (at the required tangential Mach number for the surface layer, n = N)
7. Material specific acoustic reactance at each frequency for each layer, $X_e^{(n)}(f_j)$
8. Distributed impedance and wavenumber of cavity filler (if any) at each frequency for each layer, $k^{*(n)}(f_j)$, rad/m and $z^{*(n)}(f_j)$, MKS-RAYLS/m.

9. Cavity depth of each layer, $d^{*(n)}$, m, if simple cavity configurations (see (12) below).

10. Honeycomb effective radius, $r_e^{*(n)}$, m, for each layer, if simple, small-radius honeycomb forms air-filled† cavities.

11. Kinematic viscosity of cavity medium, ν, m^2/sec, if simple, small-radius honeycomb forms air-filled† cavities.

Calculation of Cavity Impedance Matrices

12. The cavity impedance matrices are defined by

$$A^{(n)}(f_i) = \begin{bmatrix} \cos \tilde{k}^{(n)} & \tilde{z}^{(n)} \sin \tilde{k}^{(n)} \\ -\{1/\tilde{z}^{(n)}\} \sin \tilde{k}^{(n)} & \cos \tilde{k}^{(n)} \end{bmatrix}$$

where

$$\tilde{k}^{(n)} = k^{*(n)}(f_j)\, d^{*(n)}, \quad n = 1, N$$

$$\tilde{z}^{(n)} = z^{*(n)}(f_j) / \left\{ \rho_a c_a\, k^{*(n)}(f_j) \right\}, \quad n = 1, N$$

The wave numbers $k^{*(n)}(f_j)$ and distributed impedances $z^{*(n)}(f_j)$ for each layer, at each frequency are calculated with one or more of the methods outlined below, as appropriate.

a. Simple air-filled cavity:

$$k^{*(n)}(f_j) = 2\pi f_j / c_a$$

or for a small-radius honeycomb cavity

$$k^{*(n)}(f_j) = \frac{2\pi f_j}{c_a} + i \frac{(\pi f_j \nu)^{1/2}}{r_e^{*(n)} c_a}$$

and

$$z^{*(n)}(f_j) = -i(2\pi f_j / c_a)\, \rho_a c_a$$

†i. e., if the medium in all the cavities is identical acoustically to the duct medium.

b. Simple cavity filled with bulk material: $k^{*(n)}(f_j)$ and $z^{*(n)}(f_j)$ follow directly from (8).

c. Complex, locally reacting cavity geometries, curved liners configurations, etc. – the matrices $\left[A^{(n)}(f_j)\right]$ must be derived directly from measurement and/or theoretical models.

d. Extended reaction (nonpartitioned) liner configurations – the impedance calculation method must be carried out in conjunction with the solution of the duct propagation equation, which provides values for k_{zm} and m/b. In this case $z^{*(n)}(f_j)$ can be obtained from a or b above while $k^{*(n)}(f_j)$ is denoted by $k_{rm}^{*(n)}(f_j)$ and is given by (for all layers)

$$k_{rm}^{*(n)}(f_j)/k_a = k_{rm}^{(n)}(f_j)$$

$$= \left\{\left(k^{*(n)}(f_j)/k_a\right)^2 - \delta_z\, k_{zm}^2(f_j) - \delta_m\,(m/b)^2\right\}^{1/2},$$

$$n = 1,\ N$$

$$(k_a = 2\pi f_j/c_a)$$

and $k^{*(n)}(f_j)$ can be determined from a or b above; δ_z, δ_m are unity in the absence of partitioning, but $\delta_z = 0$ if the liner is axially partitioned or $\delta_m = 0$ if circumferentially partitioned.

Liner Impedance Calculation: Iteration for Sheet Material Acoustic Resistances

13. Choose an initial value for the material specific acoustic resistance for each sheet e. g.,

$$\left\{R_e^{(n)}\right\} = \begin{Bmatrix} R_e^{(N)} \\ R_e^{(N-1)} \\ \vdots \\ R_e^{(1)} \end{Bmatrix} = \begin{Bmatrix} 1.0 \\ 1.0 \\ \vdots \\ 1.0 \end{Bmatrix}$$

14. Form a value for the complex material specific acoustic impedance for each sheet at each frequency

$$\left\{ \Delta Z^{(n)}(f_j) \right\} = \left\{ R_e^{(n)} - i\, X_e^{(n)}(f_j) \right\}$$

with $\left\{ R_e^{(n)} \right\}$ from (13) or (18) and $\left\{ X_e^{(n)}(f_j) \right\}$ from (7).

15. Calculate the complex liner specific acoustic impedance at each frequency by repeated application of the following equation, starting with $\tilde{v}^{(o)}(f_j) = 0$, $\tilde{p}^{(o)}(f_j) = 1.0$

$$\begin{Bmatrix} \tilde{p}^{(n)}(f_j) \\ \tilde{v}^{(n)}(f_j) \end{Bmatrix} = \begin{bmatrix} 1 & \Delta Z^{(n)}(f_j) \\ 0 & 1 \end{bmatrix} \begin{bmatrix} A^{(n)}(f_j) \end{bmatrix} \begin{Bmatrix} \tilde{p}^{(n-1)}(f_j) \\ \tilde{v}^{(n-1)}(f_j) \end{Bmatrix}.$$

with $A^{(n)}(f_j)$ from (12). (The resulting values $\tilde{p}^{(n)}(f_j)$, $\tilde{v}^{(n)}(f_j)$ correspond to an arbitrary value of $p^{(o)}(f_j)$ and are denoted by tilde.) The liner specific acoustic impedance is given by

$$Z(f_j) = \tilde{p}^{(N)}(f_j) / \tilde{v}^{(N)}(f_j)$$

16. a. Calculate the actual, complex particle velocity Mach number at each frequency for the surface layer (n = N)

$$v^{(N)}(f_j) = 2p_o(f_j) / \left\{ Z(f_j) + 1 \right\}$$

with $p_o(f_j)$ from (5) and $Z(f_j)$ from (15).

b. Calculate the actual, complex particle velocity Mach number for all the remaining layers at each frequency

$$\left\{ v^{(n)}(f_j) \right\} = \left(\frac{v^{(N)}(f_j)}{\tilde{v}^{(N)}(f_j)} \right) \left\{ \tilde{v}^{(n)}(f_j) \right\}$$

with $\tilde{v}^{(N)}(f_j)$ from (15) and $v^{(N)}(f_j)$ from (16a).

17. Calculate the total effective particle velocity Mach number for each layer

$$\left\{v_e^{(n)}\right\} = \left\{\left[\sum_{j=1}^{N_f} \left|v^{(n)}(f_j)\right|^2\right]^{1/2}\right\}$$

with $\left\{v^{(n)}(f_j)\right\}$ from (16b).

18. Read off from $R^{(n)}[v]$ (the material D.C. flow characteristics from (6), the sheet material specific acoustic resistances corresponding to positive and negative values of the effective velocity Mach numbers from (17):

$$\left\{R_+^{(n)}\right\} = \left\{R\left[+v_e^{(n)}\right]\right\}$$

$$\left\{R_-^{(n)}\right\} = \left\{R\left[-v_e^{(n)}\right]\right\}$$

and calculate the effective specific acoustic resistances with

$$\left\{R_e^{(n)}\right\} = \left\{2R_+^{(n)} R_-^{(n)} / \left(R_+^{(n)} + R_-^{(n)}\right)\right\}$$

If each value $R_e^{(n)}$, n = 1, N differs from its previous value (or if each differs from that assigned in (13) by less than a specified tolerance then the iteration can be terminated and the required liner specific acoustic impedance is the last value calculated at (15). Otherwise the procedure must be repeated starting at (14) with the new values $\left\{R_e^{(n)}\right\}$ or a vector based on this and preceeding vectors (for example, by linear extrapolation).

Section 5
CONCLUDING REMARKS

A natural result of a review is the identification of unanswered questions. Many such questions could be raised as to why a material has a certain acoustic property, but in this paper this area has been neglected, assuming that the material property would be measured and then used to compute the liner property. This is a valid approach and is recommended as the method to be used in the future; however, it is recognized that this approach requires both the development and standardization of precise measurement techniques.

In view of the importance of flow on material properties, it is recommended that precision methods be developed for the measurement of the flow resistance of materials in the presence of flow, including the boundary layer parameters as variables. It is also recommended that methods of measuring the nonlinear acoustic impedance of materials in presence of flow be developed. This impedance measurement must be done using time-domain techniques to see if the correspondence between flow resistance and acoustic resistance is retained valid in the presence of tangential flow.

Very little is known about the way a broadband spectrum affects the apparent (linearized) properties of a material. In the present paper, an rms effective velocity was recommended because it is realized that complex spectra, or real-time information is not generally available. It is worthwhile exploring some of these questions by looking at the material and liner properties the time domain, where the nonlinear effects are easier to characterize but the geometric effects, such as liner depth, are more complicated.

The extension of the properties of linear locally reacting liners to the case of extended reaction is deceptively simple. It should be emphasized that this is not possible in the case of nonlinear liners. Further research is needed on nonlinear extended reaction liners; however, it is beyond the scope of the present paper to discuss this in detail.

Section 6
REFERENCES

1. Proceedings of a Symposium on Acoustical Duct Treatment for Aircraft. J. Acoust. Soc. Amer., Vol 48, No. 3, 1970, P 779-842.

2. A. H. Nayfeh, J. E. Kaiser, and D. P. Telionis. The Acoustics of Aircraft Engine-Duct Systems. AIAA Paper No. 73-1153, 1973.

3. H. H. Hubbard, D. L. Lansing, and H. L. Runyan. A Review of Rotating Blade Noise Technology. J. Sound Vib., Vol 19, No. 3, 1971, P 227-249.

4. Anon: Standard Method of Test for Impedance and Absorption of Acoustical Materials by the Tube Method. ASTM Standard C-384-58.

5. R. A. Scott. The Absorption of Sound in a Homogeneous Porous Medium. Proc. Phys. Soc., Vol 58, 1946, P 165-183.

6. L. L. Beranek, Ed. Noise and Vibration Control. McGraw-Hill Book Company, 1971.

7. W. K. R. Lippert. The Practical Representation of Standing Waves in an Acoustic Impedance Tube. Acustica, Vol 3, No. 3, 1953, P 153-160.

8. T. H. Melling. An Impedance Tube for Precision Measurement of Acoustic Impedance and Insertion Loss at High Sound Pressure Levels. J. Sound Vib., Vol 28, No. 1, 1973 P 23-54.

9. W. E. Zorumski and T. L. Parrott. Non-linear Acoustic Theory for Rigid Porous Materials. NASA TN D-6196, 1971.

10. B. T. Zinn. A Theoretical Study of Non-Linear Damping by Helmholtz Resonators. J. Sound Vib. 13(3), 1970 P 347-356.

11. T. H. Melling. The Acoustic Impedance of Perforates at Medium and High Sound Pressure Levels. J. Sound Vib. 29(1), P 1-65.

12. E. J. Rice. A Model for the Acoustic Impedance of a Perforated Plate Liner With Multiple Frequency Excitation. NASA TM X-67950, 1971.

13. S. Mariano. Effect of Wall Shear Layers on the Sound Attenuation in Acoustically Lined Rectangular Ducts. J. Sound Vib. 19(3), 1971, P 261-276.

14. E. J. Rice. A Model for the Pressure Excitation, Spectrum and Acoustic Impedance of Sound Absorbers in the Presence of Grazing Flow. AIAA Paper No. 73-995 and NASA TM X-71418, 1973.

15. D. L. Armstrong. Acoustic Grazing Flow Impedance Using Waveguide Principles. NASA CR 120848, 1971.

16. W. Eversman, M. D. Nelsen, D. Armstrong and O. J. Hall. Design of Acoustic Linings for Ducts With Flow. J. Aircraft 9(8), 1972, P 548-556.

17. C. Zwicker and C. W. Kosten. Sound Absorbing Materials. Elsevier Publishing Company, New York, NY, 1949.

18. K. W. Ingard and H. Ising. Acoustic Non-linearity of an Orifice. J. Acoust. Soc. Amer. 42(1), 1967, P 6-17.

19. L. S. Wirt. Analysis, Testing, and Design of Ducts. J. Acoust. Soc. Amer. 51(5), 1972, P 1448-1463.

20. U. J. Kurze and C. H. Allen. Influence of Flow and High Sound Level on the Attenuation in a Lined Duct. J. Acoust. Soc. Amer. 49(5), 1971, P 1643-1654.

21. P. M. Morse and K. U. Ingard. Theoretical Acoustics. McGraw-Hill Book Company, 1968.

22. E. Feder and L. W. Dean, III. Analytical and Experimental Studies for Predicting Noise Attenuation in Acoustically Treated Ducts for Turbofan Engines. NASA CR-1373, 1969.

23. D. Ronneberger. The Acoustical Impedance of Holes in the Wall of Flow Ducts. J. Sound Vib. 24(1), 1972, P 133-150.

24. Y. Hirata and T. Itow. Influence of Air Flow on the Attenuation Characteristics of Resonator Type Mufflers. Acoustica 28(2), 1973, P 77-132.

25. M. Budoff and W. E. Zorumski. Flow Resistance of Perforated Plates in Tangential Flow. NASA TM X-2361, October 1971.

26. J. W. Posey and K. J. Compton. Effect of Nonsymmetrical Flow Resistance upon Orifice Impedance. NASA TM X-72624, 1974.

27. T. Rogers and A. S. Hersh. The Effect of Grazing Flow on the Steady State Resistance of Square-Edged Orifices. AIAA Paper No. 75-493, March 1975.

28. D. L. Armstrong, R. J. Beckemeyer and R. F. Olsen. Impedance Measurements of Acoustic Duct Liners with Grazing Flow. J. Acoust. Soc. Amer., Vol 55, No. 6 1974.

29. P. D. Dean. An In Situ Method of Wall Acoustic Impedance Measurement in Flow Ducts. J. Sound Vib., Vol 33, No. 3, 1974, P 1-34.

30. L. S. Wirt. The Design of Sound Absorptive Materials to Meet Special Requirements. Paper Presented at 86th Meeting of the Acoustical Society of America, Los Angeles, California, 1973.

31. W. E. Zorumski. Acoustic Impedance of Curved Multi-Layered Duct Liners. NASA TN D-7277, 1973.

32. D. Edkins. Acoustically Treated Ground Tests Nacelle for the General Electric TF39 Turbofan. NASA CR-120915, January 1972.